

ANTIMATTER PRODUCTION IN HIGH ENERGY COLLISIONS*

J. CLEYMANS

UCT-CERN Research Centre

and

Department of Physics, University of Cape Town, South Africa

(Received January 2, 2012)

A short review is presented of some results related to the chemical equilibration of hadrons in the final state of p - p and heavy ion collisions. Expectations are discussed also for the production of more complex forms of antimatter like antinuclei and antihypernuclei.

DOI:10.5506/APhysPolBSupp.5.669

PACS numbers: 12.40.Ee, 25.75.Dw, 05.20.-y, 5.70.-a

1. The hadronic world

After analysing particle multiplicities for two decades a remarkably simple picture has emerged for the chemical freeze-out parameters [1,2,3]. Some of the results, including analyses from [4,5,6,7], are summarised in Fig. 1.

These fit nicely on a curve corresponding to an energy per hadron $E/N \approx 1$ GeV for all beam energies [8,9]. Most of the points in Fig. 1 (except obviously the ones at RHIC) refer to integrated (4π) yields.

The temperature at $\mu_B = 0$ is remarkably close to the original Hagedorn temperature [10,11] obtained by simply summing the number of hadronic resonances as shown in Fig. 2. A recent estimate of this temperature in [12] is given by

$$T_H = 174 \pm 11 \text{ MeV}, \quad (1)$$

as shown in Fig. 2. At higher masses the increase stops which is presumably related to the difficulty in identifying heavy hadronic resonances, a situation which will probably never be resolved experimentally.

When the temperature and baryon chemical potential are translated to net baryon and energy densities, a different, but equivalent, picture emerges, shown in Fig. 3. This clearly shows the importance of going to a beam

* Talk presented at HIC for FAIR Workshop and XXVIII Max Born Symposium "Three Days on Quarkyonic Island", Wrocław, Poland, May 19–21, 2011.

energy region of around 8–12 GeV as this corresponds to the highest freeze-out baryonic density and to a rapid change in thermodynamic parameters [13, 14].

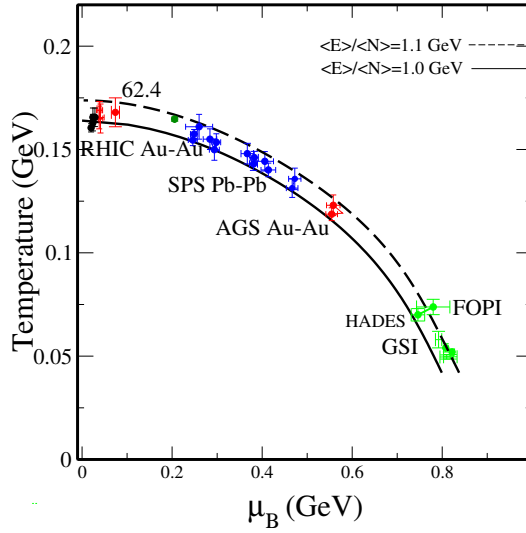


Fig. 1. Values of the freeze-out parameters obtained at beam energies ranging from 1 GeV to 200 GeV.

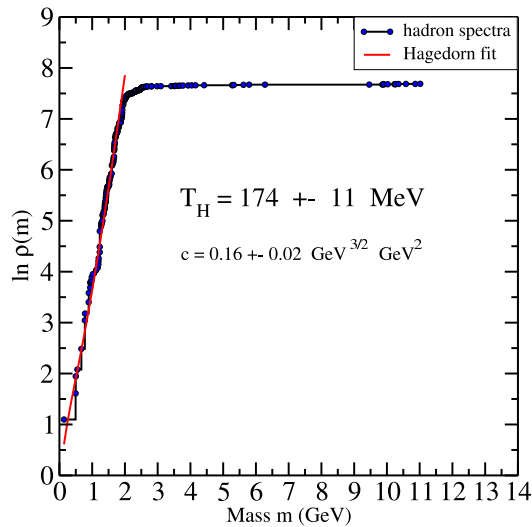


Fig. 2. Cumulative number of hadronic resonances as a function of m [12]. The hadronic data include baryons, mesons and also heavy resonances made up of charm and bottom quarks.

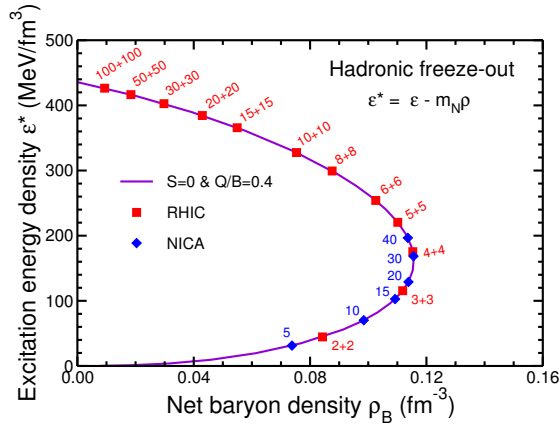


Fig. 3. The hadronic freeze-out line as obtained from the values of μ_B and T that have been extracted from the experimental data in [3]. The calculation employs values of μ_Q and μ_S that ensure $\langle S \rangle = 0$ and $\langle Q \rangle = 0.4 \langle B \rangle$ for each value of μ_B . Also indicated are the beam energies (in GeV/N) for which the particular freeze-out conditions are expected at either RHIC or FAIR or NICA.

2. Antimatter

One of the striking features of particle production at high energies is the near equal abundance of matter and antimatter in the central rapidity region [15, 16]. As is well known, a similar symmetry existed in the initial stage of the early universe and it still remains a mystery as to how this got lost in the subsequent evolution of the universe reaching a stage with no visible amounts of antimatter being present.

Closely related to this matter/antimatter symmetry is the production of light antinuclei, hypernuclei and antihypernuclei at high energies. Since the first observation of hypernuclei in 1952 [17] there has been a steady interest in searching for new hypernuclei, exploring the hyperon–nucleon interaction which is relevant (see *e.g.* [18, 19]) for nuclear physics. Hypernuclei decay with a lifetime which depends on the strength of the hyperon–nucleon interaction. While several hypernuclei have been discovered since the first observations in 1952, no antihypernucleus has ever been observed until the recent discovery of the antihypertriton in Au+Au collisions at $\sqrt{s_{NN}} = 200$ GeV by the STAR Collaboration at RHIC [20]. The yield of (anti)hypernuclei measured by STAR is very large, in particular they seem to be produced with a similar yield as other (anti)nuclei, in particular (anti)helium-3. This abundance is much higher than measured for hypernuclei and nuclei at lower energies [21]. It is of interest to understand the nature of this enhancement, and for this reason the mechanism of production of (anti)hypernuclei should be investigated.

The thermalization assumption applies successfully to hadrons produced in a large number of particle and nuclear reactions at different energies (see *e.g.* [22, 23, 24]). This fact allows us to estimate thermal parameters characterizing the particle source for each colliding system, relevant for the understanding of the thermal properties of dense and hot matter, and in particular for studies of QCD phase transitions. Using the parametrizations of thermal parameters found in the THERMUS model [25, 26], estimates have been made of the yields of (anti)hypernuclei that can be directly compared to the recently measured yields at RHIC as well as predictions of (anti)matter and (anti)hypernuclei production at the Large Hadron Collider (LHC) [27]. A similar analysis, not including p - p results, has been presented recently in [28], where it was shown that ratios of hypernuclei to nuclei show an energy dependence similar to the K^+/π^+ one with a clear maximum at lower energies. A quantitative study as to how the matter/antimatter symmetry is reached as the beam energy is increased has been presented in [27]; estimates of ratios of hypernuclei and antihypernuclei yields in Au+Au collisions at RHIC using the above mentioned parametrizations of thermal parameters that best fit hadron production at RHIC have also been presented [27]. The analysis uses a thermal model and aims to elucidate the production mechanism of hypernuclei and antihypernuclei in heavy ion collisions at RHIC and LHC energies, thus providing insight in the surprising increase of (anti)hypernuclei production at high energies.

3. Production of antibaryons

In heavy-ion collisions the increase in the antimatter to matter ratio with the center-of-mass energy of the system has been observed earlier by the NA49 [29, 30] and the STAR [31] collaborations. The trend of \bar{p}/p ratio increase with the energy towards unity is shown in Fig. 4, where the open squares refer to heavy ion collisions and the solid circles refer to p - p collisions. It includes results from the NA49 [29], STAR [31] and the new results from the ALICE Collaboration [16]. The two input parameters, the chemical freeze-out temperature T and the baryon chemical potential μ_B as a function of \sqrt{s} are taken from Ref. [3]

$$T(\mu_B) = a - b\mu_B^2 - c\mu_B^4 \quad (2)$$

with $a = 0.166 \pm 0.002$ GeV, $b = 0.139 \pm 0.016$ GeV⁻¹ and $c = 0.053 \pm 0.021$ GeV⁻³. This parametrization is similar and consistent with the one proposed in Ref. [32]. The solid line in Fig. 4 is obtained from the THERMUS model [25, 26] using T from equation (1) and μ_B from equation (2).

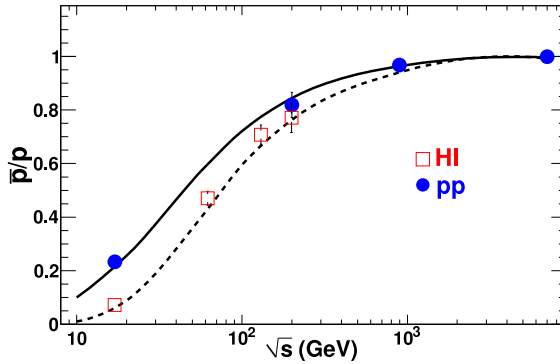


Fig. 4. The \bar{p}/p ratio as function of \sqrt{s} . The solid circles are results from p - p collisions and the open squares are results from HI collisions as a function of the invariant beam energy [15, 16, 29, 30, 31].

The solid circles represent μ_B , obtained after fitting experimental data with the THERMUS model [25, 26]. The solid line is a new parametrization adjusted for p - p collisions [27]. In view of the fact that peripheral and central collisions show no noticeable change in the temperature, the same T dependence for p - p as in heavy ion collisions was used [27] but the dependence on μ_B on beam energy is now given by

$$\mu_B = d / (1 + e\sqrt{s}) \quad (3)$$

with $d = 0.4$ GeV and $e = 0.1599$ GeV $^{-1}$ [27].

It is important to note that μ_B is always lower in p - p collisions than in heavy ion collisions, *e.g.* the freeze-out chemical potential follows a different pattern, due to the lower stopping power in p - p collisions.

The relation between the \bar{p}/p ratio and μ_B can be shown easily within the statistical concept using the Boltzmann statistics. In the calculations, the appropriate statistics and also feed-down from strong decays are taken into account. The density of particle i is then given by

$$n_i = \frac{d_i}{2\pi^2} K_2 \left(\frac{m_i}{T} \right) e^{(N_B\mu_B + N_S\mu_S)/T} \quad (4)$$

with N_B and N_S being the baryon and strangeness quantum numbers of particle i .

This leads to a \bar{p}/p ratio of (excluding feed-down from heavier resonances)

$$\frac{n_{\bar{p}}}{n_p} = e^{-(2\mu_B)/T}. \quad (5)$$

The ratio of strange antibaryons/baryons is then given by

$$\frac{n_{\bar{B}}}{n_B} = e^{-(2\mu_B - N_S\mu_S)/T}. \quad (6)$$

As μ_S is always smaller than μ_B , the ratios appear ordered with the strangeness quantum number, *i.e.* the higher N_S , the smaller the difference between antibaryon and baryon. This trend is shown in Fig. 5 comparing the results from the model with experimental data [27]. The agreement between the model results and the data is very good.

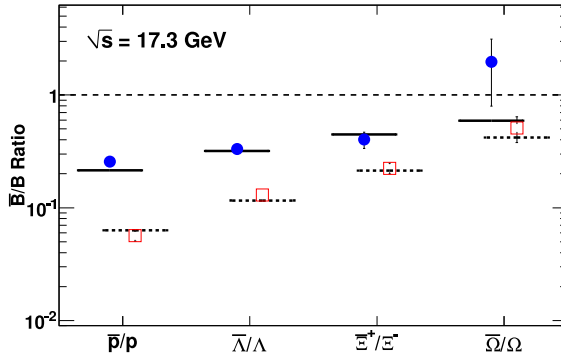


Fig. 5. Antibaryon to baryon ratios at the SPS according to strangeness content. Circles refer to p - p collisions, squares to heavy ion collisions [27].

4. Production of nuclei, antinuclei, hypernuclei and antihypernuclei

The production of light nuclei including hypertritons (${}^3_{\Lambda}\text{H}$) and antihypertritons (${}^3_{\Lambda}\bar{\text{H}}$) was recently observed by the STAR Collaboration [20]. The abundances of such light nuclei and antinuclei follows a consistent pattern in the thermal model. The temperature remains the same as before but an extra factor of μ_B is picked up each time the baryon number is increased. Each proton or neutron thus simply adds a factor of μ_B to the Boltzmann factor. The production of nuclear fragments is therefore very sensitive to the precise value of the baryon chemical potential and could thus lead to a precise determination of μ_B .

The ratios within the statistical approach using the grand-canonical formalism can be easily written, based on Eq. (4). Deuterium has an additional neutron and the antideuterium to deuterium ratio is given by the square of the antiproton to proton ratio

$$\frac{n_{\bar{d}}}{n_d} = e^{-(4\mu_B)/T}. \quad (7)$$

Helium 3 has 3 nucleons and the corresponding anti-helium 3 to helium 3 ratio is given by

$$\frac{n_{\overline{3}\text{He}}}{n_{3\text{He}}} = e^{-(6\mu_B)/T} . \tag{8}$$

If the nucleus carries strangeness this leads to an extra factor of μ_S

$$\frac{n_{\overline{3}\text{H}}}{n_{3\text{H}}} = e^{-(6\mu_B - 2\mu_S)/T} . \tag{9}$$

In mixed ratios the different degeneracy factors are also taken into account, *e.g.* 6 for ${}^3_{\Lambda}\text{H}$ and 2 for ${}^3_{\Lambda}\text{H}$

$$\frac{n_{\overline{3}\text{H}}}{n_{3\text{H}}} = 3e^{-(6\mu_B - \mu_S)/T} . \tag{10}$$

In the model like in the data the He^3 and $\overline{\text{He}}^3$ yields have been corrected for the part coming from hypertriton and antihypertriton decays assuming a decay branch ratio for the decay of 25%.

In Fig. 6 a comparison is shown of the various antiparticle/particle ratios for two different beam energies.

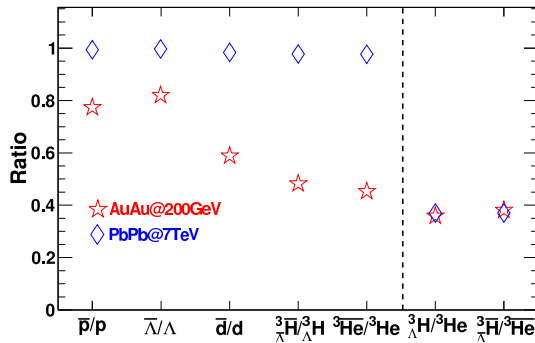


Fig. 6. Comparison of two different collision energies for heavy ion collisions [27].

5. Conclusions

The thermal model is providing valuable insights in the composition of the final state produced in heavy ion collisions and also in p - p collisions. It shows a clear systematic way of interpreting results concerning identified particles. The production of antimatter like antinuclei, hypernuclei and antihypernuclei shows a new region of applications for the thermal model which promises to be very useful.

The contributions of S. Kabana, I. Kraus, H. Oeschler, J. Randrup, K. Redlich, N. Sharma, D. Worku in the results presented here are gratefully acknowledged. This work was supported by the South Africa–Poland scientific collaboration.

REFERENCES

- [1] A. Andronic, P. Braun-Munzinger, J. Stachel, *Nucl. Phys.* **A834**, 237C (2010) [arXiv:0911.4931 [nucl-th]].
- [2] F. Becattini, J. Manninen, M. Gazdzicki, *Phys. Rev.* **C73**, 044905 (2006).
- [3] J. Cleymans, H. Oeschler, K. Redlich, S. Wheaton, *Phys. Rev.* **C73**, 034905 (2006).
- [4] R. Picha, University of Davis, Ph.D. thesis 2002.
- [5] J. Takahashi, R. Souza [STAR Collaboration], *J. Phys. G* **36**, 064074 (2009) [arXiv:0812.4157 [nucl-ex]].
- [6] T. Galatyuk *et al.* [HADES Collaboration], arXiv:0911.2411 [nucl-ex].
- [7] N. Herrmann [FOPI Collaboration], *Prog. Part. Nucl. Phys.* **62**, 445 (2009).
- [8] J. Cleymans, K. Redlich, *Phys. Rev. Lett.* **81**, 5284 (1998).
- [9] J. Cleymans, K. Redlich, *Phys. Rev.* **C60**, 054908 (1999).
- [10] R. Hagedorn, *Nuovo Cimento Suppl.* **3**, 147 (1965).
- [11] R. Hagedorn, J. Ranft, *Nucl. Phys.* **B48**, 157 (1972).
- [12] J. Cleymans, D. Worku, *Mod. Phys. Lett.* **A26**, 1197 (2011) [arXiv:1103.1463 [hep-ph]].
- [13] J. Randrup, J. Cleymans, *Phys. Rev.* **C74**, 047901 (2006).
- [14] J. Randrup, J. Cleymans, arXiv:0905.2824 [nucl-th].
- [15] B.I. Abelev *et al.* [STAR Collaboration], *Phys. Rev.* **C79**, 034909 (2009) [arXiv:0808.2041 [nucl-ex]].
- [16] K. Aamodt *et al.* [ALICE Collaboration], *Phys. Rev. Lett.* **106**, 072002 (2010) [arXiv:1006.5432 [hep-ex]].
- [17] M. Danysz, J. Pniewski, *Phil. Mag.* **44**, 348 (1953).
- [18] D. Hahn, H. Stöcker, *Nucl. Phys.* **A476**, 718 (1988).
- [19] H. Stöcker, W. Greiner, *Phys. Rep.* **137**, 277 (1986).
- [20] B.I. Abelev *et al.* [STAR Collaboration], *Science* **328**, 58 (2010) [arXiv:1003.2030 [nucl-ex]].
- [21] R. Rapp, E.V. Shuryak, *Phys. Rev. Lett.* **86**, 2980 (2001).
- [22] F. Becattini, *Z. Phys.* **C76**, 269 (1997); F. Becattini, U. Heinz, *Z. Phys.* **C69**, 485 (1996).
- [23] For general reviews see *e.g.* K. Redlich, J. Cleymans, H. Oeschler, A. Tounsi, *Acta Phys. Pol. B* **33**, 1609 (2002); P. Braun-Munzinger, K. Redlich, J. Stachel, arXiv:nucl-th/0304013v1.

- [24] P. Braun-Munzinger, J. Cleymans, H. Oeschler, K. Redlich, *Nucl. Phys.* **A697**, 902 (2002).
- [25] S. Wheaton, J. Cleymans, *J. Phys. G* **31**, S1069 (2005) [hep-ph/0412031].
- [26] S. Wheaton, J. Cleymans, M. Hauer, *Comput. Phys. Commun.* **180**, 84 (2009).
- [27] J. Cleymans *et al.*, arXiv:1105.3719 [hep-ph].
- [28] A. Andronic, P. Braun-Munzinger, J. Stachel, H. Stöcker, *Phys. Lett.* **B697**, 203 (2011) [arXiv:1010.2995v2 [nucl-th]].
- [29] C. Alt *et al.* [NA49 Collaboration], arXiv:nucl-ex/0512033.
- [30] C. Alt *et al.* [NA49 Collaboration], *Phys. Rev.* **C77**, 024903 (2008) [arXiv:0710.0118 [nucl-ex]].
- [31] B.I. Abelev *et al.* [STAR Collaboration], *Phys. Rev.* **C75**, 064901 (2007) [arXiv:nucl-ex/0607033].
- [32] A. Andronic, P. Braun-Munzinger, J. Stachel, *Nucl. Phys.* **A772**, 167 (2006).